


## RESEARCH ARTICLE

# Uncertainty reduction in residual stress measurements by an optimised inverse solution using nonconsecutive polynomials

Diego L. Brítez<sup>1</sup>  | Michael B. Prime<sup>2</sup> | Sana Werda<sup>1</sup> | Reynald Laheurte<sup>1</sup> | Philippe Darnis<sup>1</sup> | Olivier Cahuc<sup>1</sup>

<sup>1</sup>University of Bordeaux, CNRS, Bordeaux INP, I2M, UMR 5295, Talence, France

<sup>2</sup>Los Alamos National Laboratory, New Mexico, USA

## Correspondence

Diego L. Brítez, Université de Bordeaux, 351 cours de la Libération, Talence, France.

Email: [diego-luis.britez-gonzalez@u-bordeaux.fr](mailto:diego-luis.britez-gonzalez@u-bordeaux.fr)

## Funding information

I2M Laboratory of the University of Bordeaux; U.S. Department of Energy through the Los Alamos National Laboratory

## Abstract

Many destructive methods for measuring residual stresses such as the slitting method require an inverse analysis to solve the problem. The accuracy of the result as well as an uncertainty component (the model uncertainty) depends on the basis functions used in the inverse solution. The use of a series expansion as the basis functions for the inverse solution was analysed in a previous work for the particular case where functions orders grew consecutively. The present work presents a new estimation of the model uncertainty and a new improved methodology to select the final basis functions for the case where the basis is composed of polynomials. Including nonconsecutive polynomial orders in the basis generates a larger space of possible solutions to be evaluated and allows the possibility to include higher-order polynomials. The paper includes a comparison with two other inverse analyses methodologies applied to synthetically generated data. With the new methodology, the final error is reduced and the uncertainty estimation improved.

## KEYWORDS

inverse analysis, residual stress measurement, uncertainty estimation

## 1 | INTRODUCTION

Many destructive residual stress-measuring techniques are based on the relationship between the deformation measurements obtained during a sequential material removal process that releases stresses in the work specimen. Because an analytic solution in generally is not possible, an inverse solution approach is used to solve this problem.<sup>[1]</sup> In order to implement this technique, the residual stress profile (RSP) is expressed as a linear combination of a known basis functions. Multiple functions have been used in the literature such as some continuous series (the Legendre polynomials, the power functions, the Chebyshev polynomials, etc.) or pulse functions (bounded Heaviside) as the basis.<sup>[2]</sup>

Previous work carried by Prime and Hill<sup>[3]</sup> studied the solutions based on series-expanded functions by looking the optimal solution based on the total uncertainty reduction. Like most uses of a series expansion inverse, for example, previous studies,<sup>[4–6]</sup> this study considered polynomials where the orders in the basis functions vary consecutively (1, 2,

This is an open access article under the terms of the [Creative Commons Attribution](https://creativecommons.org/licenses/by/4.0/) License, which permits use, distribution and reproduction in any medium, provided the original work is properly cited.

© 2022 The Authors. *Strain* published by John Wiley & Sons Ltd.

3, 4, 5, ...). Thus, the maximal polynomial order to be included is limited by the number of strain measurements, since the degrees of freedom of the system of equations is limited by the number of measurements.

The present work looks to improve this methodology by studying a wider range of solutions. For the polynomial basis functions case, the solution is also based in the minimisation of the total uncertainty, so it can be interpreted as a generalisation of the Prime and Hill methodology,<sup>[3]</sup> for a polynomial functions case.

This is done by including combinations of nonconsecutive polynomial orders. This choice allows including higher polynomial orders in the solution. Thus, the identification and elimination polynomial terms that mostly only add noise are achieved. In addition, a new model uncertainty for the residual stresses (a total uncertainty component) is proposed and implemented. The spirit of this article is to bring new tools to analyse residual stresses. The same experimental data can be analysed by using different inverse solution methodologies; consistent results would increase the certainty of the results.

## 2 | METHODOLOGY

Different residual stress destructive measurement techniques require solution by inverse analyses. They are classified based on the part geometry and the cutting process. The principal methods that can be found in the literature are the layer removal method,<sup>[7]</sup> the hole drilling method,<sup>[8–10]</sup> and the slitting method.<sup>[2,11–15]</sup>

This section reviews the key points and the equations to solve a residual stress problem by the inverse analysis approach. Detailed information of each specific method can be found in the references.

The basic approach in all these methods is to incrementally remove material from the specimen. At each removal step, some internal stresses of the specimen are released, distorting the specimen. Two measurements are made: the depth of the cut  $a_i$  (where the  $i$  subindex refers to the cut number) and the correspondent measured strain,  $\epsilon_{meas,i}$ . The strains are measured some place where the sensitivity of the released stresses is high; the scheme of Figure 1 represents two typical strain gauge positioning (top edge and back edge) for the slitting method case. The residual stress is then calculated as function of the measured strains  $\epsilon_{meas}$ .

The series expansion solution strategy is to represent the stress profile as a linear combination of a set of known functions, called the basis functions  $P$  (in this work, only the case of polynomials will be considered). In matrix form, this is expressed as follows:

$$\{\sigma\} \approx [P][A], \quad (1)$$

where  $\sigma$  (vector with  $m$  elements) represents the RSP at each depth  $a_i$ , with  $m$  as the number of total cuts. Each column of the  $P$  (matrix with a dimension of  $m \times n$ , with  $n$  as the total number functions used) is the evaluation of each of  $n$  functions composing the basis at each  $a_i$  cut.  $A$  is a vector that is composed of the  $A_j$  function multipliers (one for each polynomial in the used in the basis). To solve the problem, a compliance matrix  $K$  (with a dimension of  $m \times n$ ) is calculated, where each element  $k_{ij}$  represents the strain that would be obtained by a stress profile  $P_j$ , when a cut of depth  $a_i$  is performed. Based on linear elasticity theory and superposition, the relationship between strains and the compliances matrix is as follows:

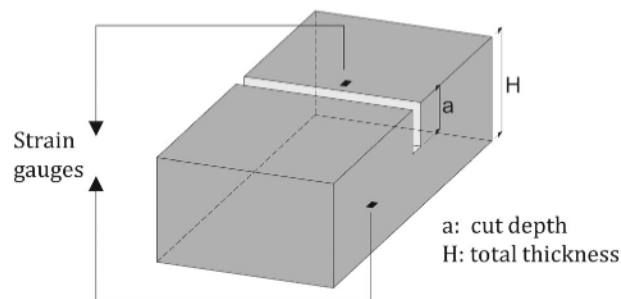


FIGURE 1 Strain gauge typical positions during strain measurement procedure for the slitting method.

$$\{\varepsilon\} = [K][A], \quad (2)$$

where the only unknown term is the multipliers vector,  $A$ . Once  $A$  is calculated by a least square fit to best approximate the measured strains,

$$\{A\} = ([K]^T[K])^{-1}[K]^T\{\varepsilon_{meas}\} = [B]\{\varepsilon_{meas}\}, \quad (3)$$

with  $[B] = ([K]^T[K])^{-1}[K]^T$ . The residual stress can be also found by applying Equation (1).

The challenge is finding a good set of basis functions  $P$  that can reproduce the RSP by applying Equation (1) with the lowest possible error.

Equations (1)–(3) allow one to calculate an estimation of the RSP based on the strains measured during the cutting process. However, they do not offer a criterion to choose the basis functions in order to obtain an optimal result. In the following, a methodology for obtaining that optimal result by minimising the total uncertainty reduction is developed.

## 2.1 | Sources of uncertainties and errors

The sources of uncertainties and the error propagation in the case of a series-expanded basis functions for residual stress-measuring process are covered in (3). In this work, a generalisation of this methodology is proposed for the polynomials basis functions case, with a modification of the model uncertainty estimation (one of the total uncertainty components).

There are two main sources of uncertainties. The first comes from the errors during the measurement process and the fitting of Equation (2) and is known as the stress uncertainty due to the strain uncertainty propagation. The second one and more complicated to estimate is associated with the capacity of the basis functions to actually reproduce the stress profile, and it is known as model error.

The total variance is then calculated by the following:

$$\Delta\sigma_{total,i}^2 = \Delta\sigma_{\varepsilon,i}^2 + \Delta\sigma_{model,i}^2 + \Delta\sigma_{F,i}^2 + \dots \quad (4)$$

where  $\Delta\sigma_{\varepsilon}$  represents the stress uncertainty due to the strain uncertainty propagation,  $\Delta\sigma_{model}$  is the model error and  $\Delta\sigma_F$  any other significant source of uncertainty not covered in this work.

The best possible solution can be based on the minimum total uncertainty, the solution giving the optimised compromise between all the sources of uncertainties.

### 2.1.1 | Strain error/uncertainty identification and propagation

For the case of the stress uncertainty due to the propagation of the strain uncertainty, the same methodology developed by Prime and Hill<sup>[3]</sup> is used in this work. Thus, only the key points are highlighted. The strain error propagation can be defined by the following:

$$\Delta\sigma_{\varepsilon,i}^2 = u_{A_1}^2 \left( \frac{\partial\sigma_i}{\partial A_1} \right)^2 + u_{A_2}^2 \left( \frac{\partial\sigma_i}{\partial A_2} \right)^2 + \dots + 2u_{A_j A_r}^2 \left( \frac{\partial\sigma_i}{\partial A_j} \right) \left( \frac{\partial\sigma_i}{\partial A_r} \right), \quad (5)$$

where  $\Delta\sigma_{\varepsilon,i}$  is the stress uncertainty at the  $a_{i,th}$  position and  $u_{A_j}$  is the uncertainty in the parameter  $A_j$ .

From Equation (1),

$$\frac{\partial \sigma_i}{\partial A_j} = P_j(x), \quad (6)$$

then Equation (5) can be written in its matrix form as follows:

$$\{\Delta \sigma_\varepsilon\}^2 = \text{diag}([P][V][P]^T), \quad (7)$$

with  $V$  representing the covariance matrix of the  $u_{A_j A_r}^2$  terms and  $\text{diag}$  indicates a vector formed by the diagonal elements of the matrix. The covariance matrix can be calculated by the following:

$$[V] = [B][\text{DIAG}[u_\varepsilon]^2][B]^T \quad (8)$$

where  $u_{\varepsilon,i}$  are the strain uncertainties values; in this case,  $\text{DIAG}[u_\varepsilon]$  indicates a diagonal matrix with the  $u_{\varepsilon,i}$  elements as the diagonal elements.

There are two possibilities in order to estimate the strain uncertainty. The first one is the uncertainty due to the inherent precision of the experimental apparatus (in which its root mean square [rms] value is represented by  $\bar{e}$ ). The second is an estimation based on the strain misfit and the degrees of freedom of the system  $u_{\varepsilon_{mf,i}}$ .

To be conservative, the maximum of those two possibilities is used at each cut depth:

$$u_{\varepsilon_i} = \max(e_i, u_{\varepsilon_{mf,i}}), \quad (9)$$

where  $u_{\varepsilon_{mf}}$  represents the strain uncertainty due to the strain misfit.

The rms misfit uncertainty  $\bar{u}_\varepsilon$  is calculated by the rms mean is calculated as follows:

$$\bar{u}_\varepsilon = \sqrt{\frac{1}{m-n} \sum_{i=1}^m u_{\varepsilon_i}^2}, \quad (10)$$

which gives the individual uncertainty of the strain uncertainty due to the strain misfit at each cut:

$$u_{\varepsilon_{mf,i}} = \sqrt{\frac{m}{m-n}} |\varepsilon_{\text{meas}_i} - \varepsilon_{\text{calc}_i}|. \quad (11)$$

Once the strain uncertainty is identified,  $\bar{u}_\varepsilon$ , the correspondent stress uncertainty component can be calculated by applying Equation (7).

### 2.1.2 | Model error/uncertainty

The second uncertainty component considered in this equation is the model error. In order to explain it, Equation (1) is considered.

Each polynomial  $P_j$  in the series may be seen as a unique source of information (unavailable in other polynomials for the case of an orthogonal basis). In the hypothetical case of a perfect fit of the multipliers  $A$ , the more polynomials used in the series, the closer the approximation to the stress profile will be. But the number of available data is limited to  $m$  values (the number of cuts). The maximum number of polynomials to be fitted is also limited to this value.

Considering the strain uncertainty given in Equation (11), if the number of polynomials (represented by  $n$ ) used to fit the RSP is equal to the number of available data  $m$ , the strain uncertainty will tend to infinity. The associated stress uncertainty component also will tend to infinity.



This fact forces reducing the number of polynomials used in the series. This truncation reduces the capacity to accurately reproduce the stress profile. The uncertainty associated to this mathematical phenomenon is known as the model uncertainty.

### Model uncertainty estimation

The model uncertainty cannot be calculated directly because the real stress profile is not known, so it can only be estimated based on hypotheses. In the Prime and Hill methodology,<sup>[3]</sup> this estimation is made based on the hypotheses that the uncertainty is the standard deviation of a set of solutions considered similar to each other:

$$\Delta\sigma_{\text{model},i}^2(q) \approx \frac{1}{N-1} \sum_{k=b}^c (\sigma_{k,i} - \bar{\sigma}_i)^2, \quad (12)$$

where the  $i$  sub index refers that the calculation is made for a cut depth  $a_i$  and  $b$  and  $c$  are solution identifiers where their values represent the maximal polynomial order in the considered solution. The parameter  $q$  is the solution identifier for which model error is computed, also representing the maximum order in this series composition. The subset of solutions used to estimate the error is such that  $b \leq q \leq c$ .  $N$  is the number of total solutions considered in the set (from  $b$  to  $c$ ); the use of  $N = 3$  so,  $b = q - 1$  and  $c = q + 1$  show a reasonable compromise between small and large ranges of solutions.<sup>[3]</sup> Finally,  $\bar{\sigma}_i$  is the mean solution in the considered range from  $k = b$  to  $c$ .

In this work, a new algorithm is going to be presented in a later section using a larger number of potential solutions. In this case, a new estimation hypothesis is taken into account, expressed by the following:

$$\Delta\sigma_{\text{model},q_i}^2 \approx \frac{1}{r-1} \sum_{j=1}^r (\sigma_{q,i} - \sigma_{j,i})^2, \quad (13)$$

where  $r$  is the total number of solutions considered to estimate the uncertainty,  $q$  and  $j$  are basis identifiers, where  $q$  represents the particular evaluated basis solution and  $j$  all the basis solution set.

In this modelling, the uncertainty is estimated by the rms difference of the considered solution (identified by  $q$ ) and all the solutions in the set. With this new methodology, a different model uncertainty can be obtained for each solution in the set considering the same set of possible solutions.

## 2.2 | New algorithm motivation

When using consecutive polynomials as the basis function, the set with three polynomials is composed of the polynomials of order 2–4 (without considering the linear function), the set with four polynomials by 2–5 and so on. This approach implicitly limits the maximum exponential order to be used, as it demands a big number of polynomials in order to reach a high exponential order ( $[2,3,\dots,m]$ ). As previously discussed, a high number of polynomials in a solution set will increase the strain misfit uncertainty.

There are cases, for example, the additive manufacturing process, where the RSP shows cyclical peaks and valleys<sup>[16]</sup> as a result of the cyclic thermomechanical manufacturing process. The fitting of these kind of profiles would not be possible by using only polynomials with low orders.

In other cases, numerical simulations and experimental results show that when the loading process and the part geometry are symmetric in relation to the midplane of the part, the resulting residual stress are symmetric as well,<sup>[17,18]</sup> for example, sheet rolling process. On the other hand, for a symmetrical part with an antisymmetrical loading, as, for example, a bending test,<sup>[3,19]</sup> the RSP shows a tendency to be antisymmetrical. It may be expected for a symmetrical stress profile to be well represented mostly by a linear combination of even functions and for the case of an antisymmetrical function by odd functions.

Considering these particular cases, it is possible to assume a general hypothesis that when taking consecutive expansion orders in the solution set, there may be many polynomials with low contributions or even that introduce noise to the result. Furthermore, the presence of a polynomial with low contribution consumes available information, raising the strain misfit uncertainty (Equation 8) and limiting the maximum exponential order to be evaluated.

If these polynomials with low influence are not considered, it will allow the addition of other polynomials potentially with a higher and better impact on the final solution. To achieve these benefits, an algorithm looking for the smallest total uncertainty in a larger space of possible solutions is presented.

The methodology will analyse all possible solutions combination of polynomials without requiring sequential ordering and take as the final choice the one that minimises the total uncertainty given by Equation (4). The principal challenge results in identifying the sets that are going to be considered in order to estimate the model uncertainty described in Section 2.1.2.1

## 2.2.1 | The space of possible solutions

Before introducing the new algorithm, it is important to define the space searched for solutions. As in Equation (1), the RSP is represented by a finite series of known functions. The minimum and maximum numbers of polynomials used in the series as well the polynomials orders considered define and bound the space of solutions. According to Equations (1) and (2), the RSP can be evaluated if the measured strains and the polynomials composing the series are known.

The number of possible solutions to be analysed is only going to be limited by the associated computational cost, which will be governed by the following parameters:

**{Q} Possible orders list:** A 1D-array containing all the polynomial orders to be considered to include in the basis to be analysed. Example:  $\{Q\} = [2,3,\dots,21,22]$ . Normally, all orders between the bounds should be considered. The lower bound is known as **the minimum polynomial order** and the superior bound as **the maximum polynomial order**.

$p_{max}$ : A scalar value representing the maximum number of polynomials to be included in a solution basis. The calculation cost also grows significantly as this parameter is big.

$p_{min}$ : A scalar value representing the minimum number of polynomials to be evaluated in a solution basis, this parameter is normally be set at 2 or 3.

**Family of solutions:** The solutions are going to be grouped by the number of polynomials  $p$  composing their basis, where  $p_{min} \leq p \leq p_{max}$ ; these groups of solutions are called family of solutions.

Other definitions and variables obtained as a function of the previous mentioned are as follows:

**{B<sub>oc</sub>}** Basis orders composition: A 1D- array containing the polynomial orders of a basis for a particular solution. Example:  $B_{oc} = [2,3,8,15]$ , the basis of the solution being analysed is composed of the polynomials of orders 2, 3, 8 and 15.

Considering a particular family of solutions with  $p$  polynomials and all the possible polynomials orders to be combined in the basis, represented in  $\{Q\}$ , the number of possible solutions in the  $p^{th}$  family is given by the following:

$$N^o \text{ of solutions with } p \text{ polynomials} = C_{NQ}^p = \frac{NQ!}{p!(NQ-p)!}, \quad (14)$$

where  $NQ$  is a scalar representing the total number of elements in  $\{Q\}$ .

Now considering all the families of solution from  $p_{min}$  to  $p_{max}$ , the total number of solutions to be computationally evaluated is going to be given by the following:

$$\text{Total possible solutions} = C_{NQ}^{p_{min}} + C_{NQ}^{p_{min}+1} + \dots + C_{NQ}^p + \dots + C_{NQ}^{p_{max}-1} + C_{NQ}^{p_{max}} \quad (15)$$

A combinatorial algorithm of the elements found in  $Q$  combined in sets of  $p$  should be applied in order to identify every single basis order composition  $\{B_{oc}\}$ .

## 2.2.2 | General sorting algorithm description

The algorithm consists of three sorting steps before choosing the solution giving the minimum total stress uncertainty; a general chart of the algorithm is presented in Figure B1 in the Appendix.

As presented, the total uncertainty is mainly composed of two components: the stress uncertainty due to the strain uncertainty and the stress uncertainty due to the model error. The first component can be calculated directly with the measured strains and the basis functions. The second component is more complicated; each residual stress solution candidate needs a subset of possible solutions to be compared with, in order to estimate the evolution of model error. Therefore, the final problem comes down to identifying which possible solutions should be considered in the final subset to obtain a good estimation of the model uncertainty.

The procedure was developed through extensive trial and error to optimise a solution between the sometimes-competing goals of an accurate solution and an accurate uncertainty estimate. Most of the solutions inside the declared space will give poor answers; they need to be identified and eliminated. This action will help not only to find the best possible answer but also to correctly estimate the uncertainty.

As explained before, solutions with low number of polynomials should be considered in the model uncertainty estimator, but for combining reasons, the number of these solutions is lower than those solutions with a large number of polynomials. This fact would reduce their influence in the final uncertainty estimator to a minimum. In order to avoid this problem, only one solution for each family of solutions is going to be considered. This guarantees the same weight for each family in the final model uncertainty estimator.

The first and second sorting steps serve to identify the best possible solution in each family. The third sorting step eliminates solutions that may cause overestimation of the model uncertainty. The final step chooses the best remaining solution.

### 2.2.3 | First sorting procedure

The first step is to generate every single stress solution in the space of solutions and its corresponding uncertainties due to strain uncertainty  $\{\Delta\sigma_\varepsilon\}$  (given by Equation (7)). Each solution is then grouped in its family of solutions.

A significant number of the evaluated solutions will present a large strain uncertainty. In order to reduce the number of solutions to be included in following computational steps, a first sorting procedure based on  $\overline{\Delta\sigma_\varepsilon}$  (the mean value of each  $\{\Delta\sigma_\varepsilon\}$ ) is carried on. Only a fixed number of solutions in each family are going to be kept inside each family of solutions. The number of possible solutions with the lowest ( $\overline{\Delta\sigma_\varepsilon}$ ) to be kept on each family is given by a new parameter  $NP$ . A good range for this parameter is  $8 \leq NP \leq 11$ . After several tests, not included in this work, it was found that the influence of the choice of the value of  $NP$  is low when maintained in this range. The final answer has a low dependence on this parameter because this first step represents coarse filtering.

### 2.2.4 | Second sorting procedure

The purpose of the second sorting procedure is to reduce each family of solutions to only one possible solution. The idea is to calculate the total uncertainty for each possible solution in the group. The model error will be computed considering only the rest of the solutions of the family group, applying Equation (13). Then the total uncertainty (Equation (4)) and the correspondent mean total uncertainty are calculated for each candidate for the RSP. The solution 'representing' the family group in the subsequent stage is the one with the lowest total uncertainty.

### 2.2.5 | Third sorting procedure

At this point, only one solution candidate remains for each family. The model uncertainty for each solution should be recalculated, where the comparison set of solutions is the remaining solutions, with different numbers of polynomials in the basis, as the comparison set for the application of Equation (13). Once the model uncertainty has been recalculated, the total uncertainty can be updated, again by Equation (4).

The main objective of this step is to reduce the overestimation of the total stress uncertainty generated by the model uncertainty component. The overestimation is caused by the presence of solutions in the comparison set that differs greatly from the reference result.

This is caused either by the addition of noise in particular solutions (normally when there are too many polynomials in the solution) or by a lack of information (more polynomials are required in the series to generate an accurate



answer). The solution giving the minimum total uncertainty is taken as the reference solution  $\sigma_{ref}$  for the sorting procedure. The rms difference (mean value of all the measurement points) between a possible solution  $r$  and the reference is evaluated as follows:

$$\overline{\Delta\sigma_{rms,r}} = \sqrt{\frac{1}{m} \sum_{j=1}^m (\sigma_{ref,j} - \sigma_{r_j})^2}, \quad (16)$$

then, a particular solution is going to be kept in the set of possible solution if:

$$\overline{\Delta\sigma_{rms,r}^2} < \alpha \overline{\Delta\sigma_{ref,total}^2}, \quad (17)$$

where  $\overline{\Delta\sigma_{ref,total}^2}$  is the mean total uncertainty of the reference solution and  $\alpha$  a parameter that controls the sorting process. A value of  $\alpha$  equal to 1 would eliminate on average half of the possible solutions, a high number (bigger than 3 for example) would eliminate few or even no possible solutions.

A value of  $\alpha$  in the range  $1.5 \leq \alpha \leq 2$  offers the advantage of eliminating only those solutions that have a significant difference compared with the reference.

### 2.2.6 | Final solution

The elimination of some possible solutions in the previous step will modify the model uncertainty for all the solutions in the set, this may modify the solution giving the minimal final total uncertainty. As in the previous steps, the optimal result is found by the calculation of the solution with the lowest total uncertainty.

## 2.3 | Parameters value justification

There are six parameters that control the algorithm: the minimum number of polynomials ( $p_{min}$ ), the maximum number of polynomials ( $p_{max}$ ), the maximum polynomial order, the minimum polynomial order, the number of polynomials to keep after the first sorting ( $NP$ ) and the final sorting severity parameter  $\alpha$ .

The sensitivity of the final result to each parameter will depend on each particular problem. Nevertheless, it is possible to review how each one of these parameters may affect the result and justify the recommended values.

First four parameters, as studied before, control the space of solutions to be analysed. The wider the space of solutions defined, the higher the possibility of obtaining a result with reduced error and low overall uncertainty. Low polynomials orders normally have an important influence as shown by the high multiplier values, for this reason they should be always considered. This is achieved by setting the lowest polynomial order to 2 or 3. On the other hand, higher polynomial orders can help to reduce error in presence high stress gradients. The parameter controlling this limit is the maximum polynomial order. Section 3.3.1 studies this computational cost growth as function of with this parameter.

A solution with a low number of polynomials will normally be composed of low polynomials orders. As a consequence, a high stress gradient region may not be captured, increasing the error. Nevertheless, these solutions have a noise filtering capacity and they may capture the stress profile when this profile is not complex. Furthermore, these solutions contribute to a good model uncertainty estimation, and they are obtained with minimal computational cost. For these reasons, the minimum number of polynomial parameter ( $p_{min}$ ) should not be set greater than 3.

The last parameter defining the space of solution to analyse is the maximum number of polynomials ( $p_{max}$ ). Adding new polynomials to the series (usually with high polynomial orders with low contribution) can help to reduce error. At the same time, this augmentation in the number of polynomials results in an increase in the strain uncertainty propagation (this effect is seen in Figure 5 and in Figures A1 to A9), increasing the overall uncertainty estimation. The growing rate of this uncertainty component is a function of the number of data available and the noise level. High values of this parameter will increase the computational cost. For all these reasons, the minimum recommended value for this parameter is 9, in order to generate enough solutions (families) for the final model uncertainty estimation. The maximum value of this parameter is a compromise between the computational cost, the noise and the maximum polynomial order.



The number of polynomials to sample each family is given by the NP parameter. It has an impact only in the first sorting stage. Values inside the recommended range should yield the same solution or a similar result. Such values are enough to create a model error inside each family. Once the first sorting stage is completed, this parameter has no impact on the final result.

The parameter  $\alpha$  controls the severity of the last sorting. After the second sorting, the result showing the lowest overall uncertainty may result in overestimated uncertainty. This is caused by the presence of solutions in the comparing set of solutions with a large misfit compared to the reference solution.  $\alpha$  serves to judge whether this misfit is big enough to eliminate a particular solution from the final set. A value of  $\alpha = 1$  would be severe case, only those solutions found in the uncertainty region of the reference solution would rest, risking to underestimate the uncertainty. A value over 3 would give a wide range, it would only eliminate solutions if the misfit is way too big, but normally it would not eliminate any solution at all. For this reason, authors recommend some point in between these two extremes.

### 3 | BENCHMARK APPLICATION

#### 3.1 | Benchmark problem presentation

In order to evaluate the algorithm, a numerical example is carried out that consist in four different steps:

The first step consists of the generation of a RSP from a numerical simulation performed in Abaqus/Standard. The RSP is then fitted to a polynomial series in order to obtain an analytical expression. During the second step, the RSP is used to simulate the strains that would obtained at the back edge of the rolled plate when the slitting method through the thickness is applied as described in.<sup>[2,11,13,14]</sup> The third step is to generate a compliance matrix by using Cheng et al. equations<sup>[2]</sup> with the Legendre polynomials ( $L_p$ ) defined from 0 to 1 (normalised thickness), with orders from 2 to 25. This way 2 and 25 represent the minimum and maximum orders to be evaluated. Each column of the matrix represents the evaluation of a different  $L_p$ , and each line the lecture of the strain for a different depth in the cutting procedure. Finally, in the fourth step, the presented methodology is applied to the 12 sets of data (11 with random noise, detailed in Table 1 and the noiseless strain set), and the results are compared with two different methodologies, one described by Prime–Hill using polynomials<sup>[3]</sup> and the other one by Olson et al. using pulse regularisation<sup>[20]</sup>, this last method presents the advantage that is always possible to approximate a curve with the mean value in between two points of the given curve, as long the interval is small enough.

In order to break the possible dependence of the generated strains and the reconstructed because of they are generated by the same basis, an unrealistic level of noise is going to be added in 11 sets to analyse.

#### 3.2 | Data generation

##### 3.2.1 | Stress profile data generation

A numerical simulation of cold rolling process is used to generate a RSP on a steel plate with a final thickness of 16 mm. The RSP is then fitted to a polynomial series in order to obtain an analytical expression of the profile.

The analytical fitted RSP are expressed in MPa and present a mean misfit of 1% related to the numerical simulation (Figure 2). The resulting polynomial series is obtained by a linear combination of 29 Legendre polynomials (normalised thickness from 0 to 1), which orders and multipliers are given in Table 1. The main advantage of using the Legendre polynomials ( $L_p$ ) for the fitting procedure is that any stress profile represented by a linear combination of  $L_p$  where the polynomials orders are  $\geq 2$  will satisfy force and momentum equilibrium.

##### 3.2.2 | Strain data generation

This analytical expression allows one to simulate the slitting method using the equations developed by Cheng et al.<sup>[2]</sup> and thus obtain synthetic strains. The strains are obtained at the back edge of the plate, during an incremental slit cutting of 35 equal spaced cuts of 0.44 mm depth. Experimental procedures successfully carried out show that it is possible to obtain incremental slits depth as small as 0.05 mm.<sup>[16]</sup>

TABLE 1 Legendre polynomials orders and corresponding multipliers

Polynomial order	Multiplier	Polynomial order	Multiplier	Polynomial order	Multiplier
2	-199.65	14	-30.32	28	-5.997e-03
4	363.84	15	-6.98	29	-5.285e-04
5	-3.93	16	-23.78	31	1.503e-05
6	42.53	17	-4.69	33	-1.141e-06
7	-4.31	18	-0.48	34	-1.352e-08
8	117.78	21	3.12	36	1.619e-09
9	0.17	23	4.58	37	3.086e-10
10	12.59	24	-3.60	65	1.147e-30
12	-17.07	25	0.55	82	1.313e-44
13	-4.61	26	0.16		

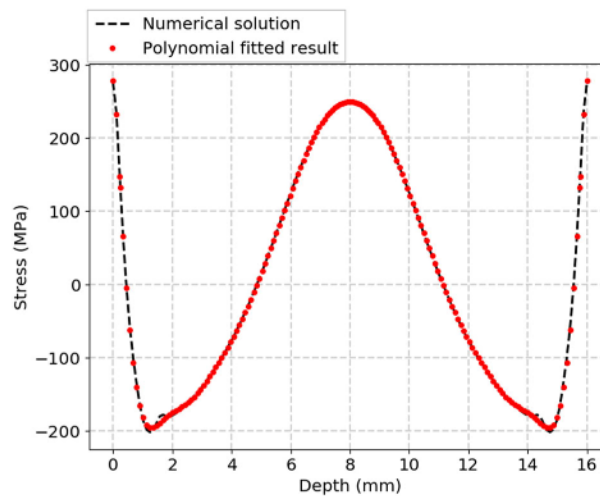


FIGURE 2 Numerical simulation and fitted polynomial stress profile.

In order to simulate real measuring conditions, 11 sets of random noise are added to the synthetic strains. A comparison of the noiseless and noise random added strain data is presented in Figure 3 for one example. The description of the mean standard deviation of each set is presented in Table 2. These levels of noise are considerably high compared with those obtained experimentally with good practice.<sup>[20]</sup> For the uncertainty calculation, an inherent error of the measuring device equal to  $2\mu\epsilon$  has been considered in all cases.

### 3.3 | Results and discussion

The individual  $i_{th}$  error is evaluated as the absolute difference between the real stress profile and the calculated stress at the measuring point. For the evaluation of the entire profile, the mean error is considered and compared with the mean total uncertainty.

For the case without noise (set 12), Figure 4 shows how the methodology sensitivity captures the error by the estimation of the model uncertainty. Without noise, only model errors are significant. Figure 4a represents the situation before the last sorting step. At this point the uncertainty overestimates real error. For this particular case, the solutions with 3 and 4 polynomials represent the solutions with higher uncertainty (and also with greater error). After the last sorting step is applied using a sorting parameter  $\alpha = 1.5$  (which is going to be used for all the cases), these two polynomials are eliminated and the overestimation is reduced obtaining a high correlation with the real mean errors. This result is presented in Figure 4b.

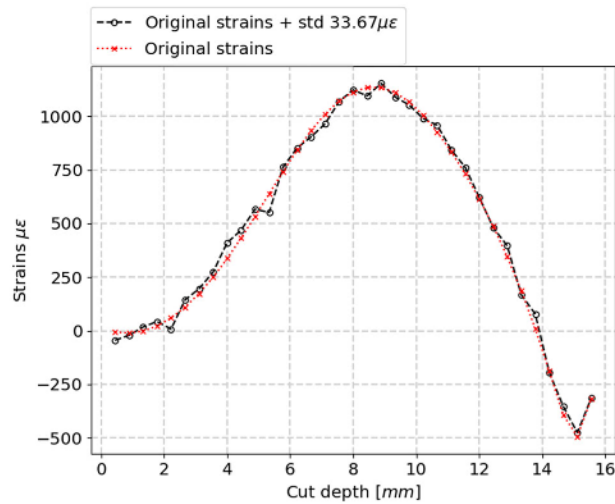


**FIGURE 3** Comparison between the synthetic strains and the ones with a random noise (set 1).

**TABLE 2** Results

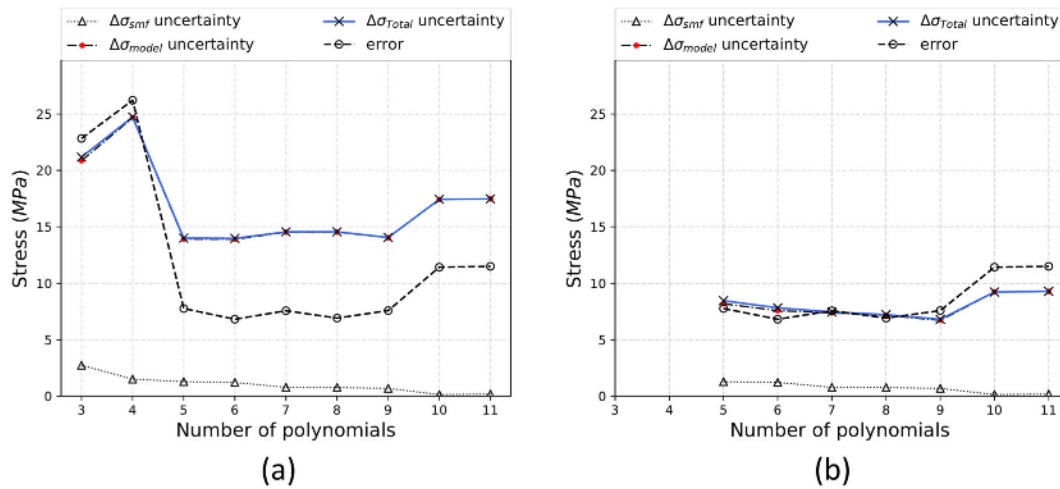
Set no.	Mean noise ( $\mu\epsilon$ )	Proposed method		Prime–Hill method		Olson et al. method	
		Uncertainty accuracy (%)	Mean error (MPa)	Uncertainty accuracy (%)	Mean error (MPa)	Uncertainty accuracy (%)	Mean error (MPa)
1	33.67	80.00	11.49	34.28	23.33	65.71	20.14
2	39.63	74.29	24.18	37.14	27.2	51.42	25.04
3	41.05	71.43	26.86	62.86	22.91	60	25.24
4	33.39	60.00	24.27	51.43	23.63	68.57	22.28
5	41.39	97.14	7.43	51.43	25	60	26.48
6	41.66	8.57	51.29	40	28.63	68.57	23.76
7	46.89	57.14	22.25	57.14	23.03	65.71	24.88
8	43.67	94.29	7.87	51.42	25.35	68.71	23.51
9	42.44	54.29	22.18	42.86	26.7	57.14	27.04
10	38.83	68.57	22.57	60	23.35	80	18.5
11	45.11	60.00	22.16	22.86	31.73	65.71	23.68
12	0	80	7.59	71.42	11.48	45.71	12.28

Figure 5 carries out the same analysis but this time with a noise-added set of data, in this particular case, set number 3. In Figure 5a, the total uncertainties estimations with a low number of polynomials (between 3 and 7) show a significant difference compared with the real error. For these possible solutions, the model uncertainty is the main component of the total uncertainty. This overestimation is due to the consideration of possible solutions with high noise levels (solutions with 10 and 11 polynomials). As the model error is a ‘comparison’ with other possible solutions, considering noisy solutions in the comparison test increases the estimation.

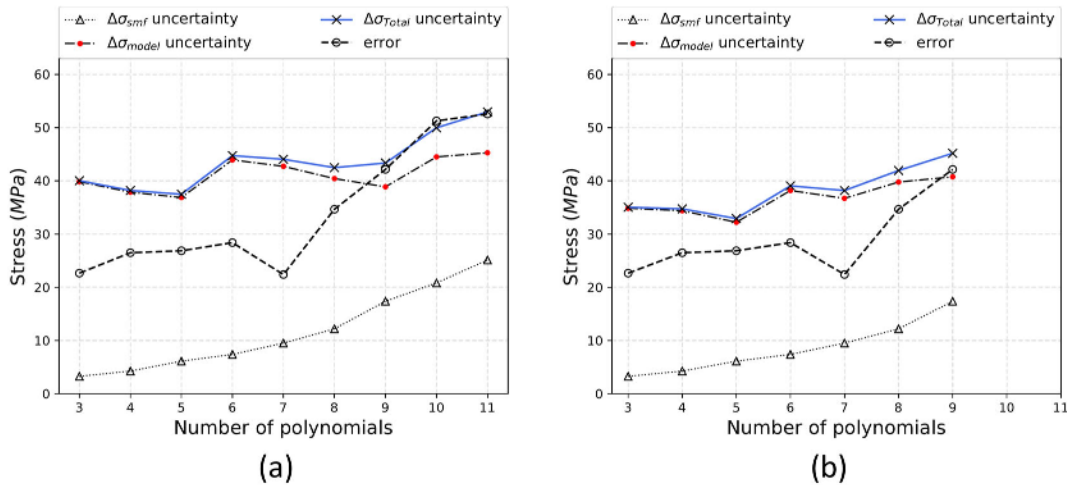
After applying the last sorting algorithm, solutions with 10 and 11 polynomials are eliminated from the comparison set (for the particular case of set 3) as shown in Figure 5b. This has an effect on the model uncertainty estimation. The total uncertainty is minimised by using five polynomials. In this case, its value and the mean absolute error are close to each other: 32.92 and 26.86 MPa, respectively (Figure B1).

Table 2 summarises the results obtained for each different set with the new proposed method and two reference methods; Prime–Hill<sup>[3]</sup> and Olson et al.<sup>[20]</sup> The uncertainty level of accuracy is measured as the fraction of the real stresses that fall into the calculated uncertainty. For the one standard deviation uncertainties presented here, 68% of the results should fall within the uncertainty. A number over 68% percent would represent a conservative





**FIGURE 4** Solution for data set 12. (a) Mean error, mean total uncertainty and its components as a function of the number of polynomials used before the last sorting process for the data set 12. (b) Mean error, mean total uncertainty and its components as a function of the number of polynomials used after the last sorting process for the data set 12.



**FIGURE 5** Solution for data set 3. (a) Mean error, mean total uncertainty and its components as a function of the number of polynomials used before the last sorting process for the data set 3. (b) Mean error, mean total uncertainty and its components as a function of the number of polynomials used after the last sorting process for the data set 3.

overestimation of uncertainty. Under 68% would underestimate uncertainty and could be dangerously nonconservative if the stresses were used to inform a structural integrity decision.

When applying the Olson et al. methodology to estimate the model error, given the high level of noise, the maximal allowed strain misfit parameter was set at  $400\mu\epsilon$  in order to obtain an acceptable regularisation and R (the span controller parameter) was 1.0; the other parameters of this methodology were kept as recommended in Olson et al.<sup>[20]</sup>

In order to evaluate the different methodologies, the average (considering the 12 samples) of the mean error through the thickness and the average mean uncertainty for each method are considered. The Prime–Hill method presents an average mean error of 24.4 MPa and an average uncertainty accuracy 46.49%. The Olson et al. methodology results show a slightly improvement in the average error (22.7 MPa) but a significant improvement in the uncertainty estimation, 63.1%. Finally, the proposed method shows the lowest average mean error (20.8 MPa) and the highest uncertainty accuracy average 67.14% including set 6 and 72.46% not including it. It should be considered that these results were obtained with a high level of noise. Nevertheless, further studies should be carried out to verify the consistency of the proposed methodology in different situations. A representative case of the results obtained with set 3 of the stress profile with its uncertainties compared with the original stress profile is presented in Figure 6.

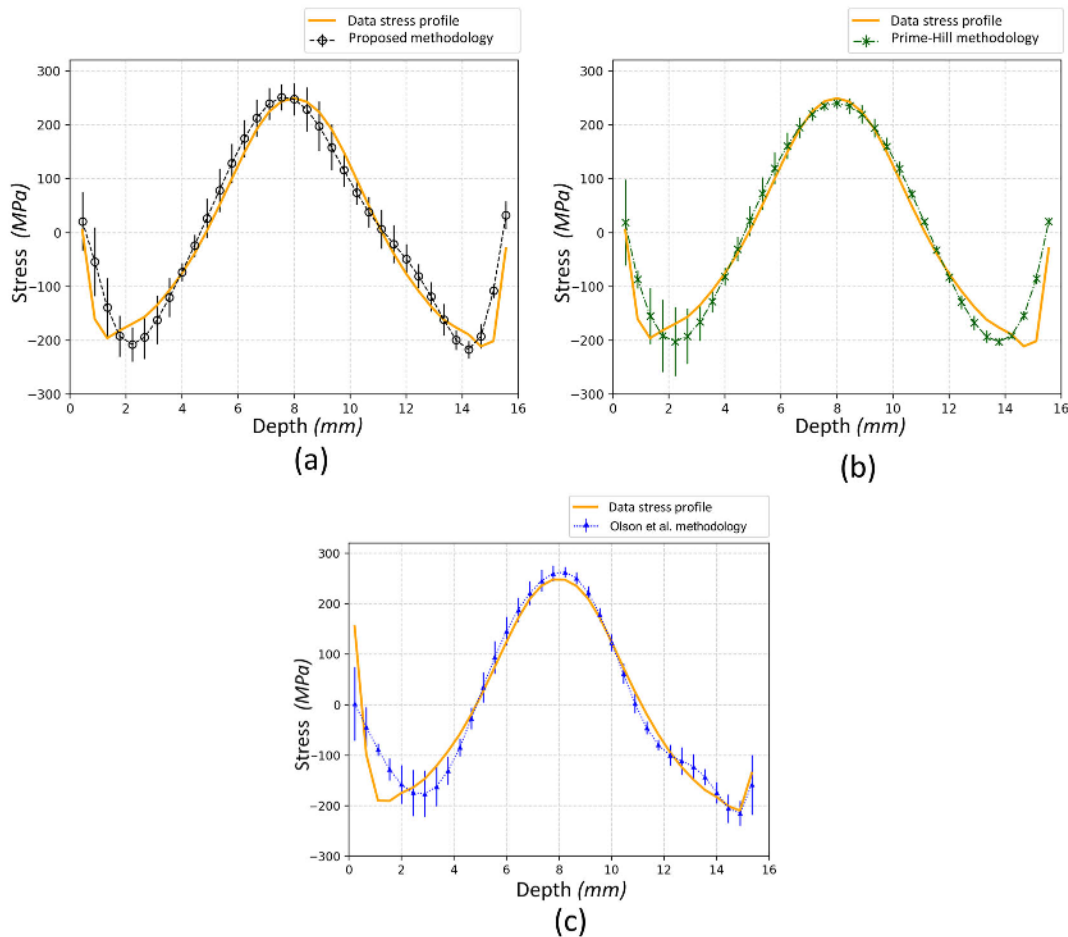


**FIGURE 6** Set 3 residual stresses solutions. (a) Proposed methodology solution. (b) Prime–Hill methodology solution. (c) Olson et al. methodology solution.

The case of set 6 is interesting. The Prime–Hill result presents a similar behaviour compared with those obtained with other sets: low error compared to the noise level but underestimated uncertainty. The methodology with pulses and regularisation gives the lowest error answer within the three methodologies. Finally, for this only for this particular data set, the proposed methodology data set shows significantly nonconservative results. The results of the particular case of the data set 6 are shown in Figure 8.

This phenomenon can be understood through an analysis of Figure 7. Figure 7a shows the mean error and uncertainties before the third sorting procedure and Figure 7b after this sorting. The solutions with the closest mean total uncertainty are solutions composed between 7 and 11 polynomials, which are the solutions that actually have the greatest error. The solution with the lowest total uncertainty corresponds to the solution with eight polynomials (therefore, the reference solution for the last stage), while the one with the lowest error corresponds to the solution with six polynomials.

The sorting process eliminates the solutions with the highest uncertainty difference compared with the reference solution (eight polynomials solution) by applying the criteria given in (17). Therefore, the solutions composed of 3, 4 and 5 are eliminated (which are the ones that actually present the lowest error) from the possible solutions set.

The measurement methodologies based on the approximation to a set of functions are subject to the choice of certain parameters that regulate the performance of each method. In the case of the Prime–Hill methodology, it is the number of polynomials in the set to be compared and the fact of taking consecutive orders. In the Olson et al. methodology, they are the maximum strain misfit allowed and the span of solutions regulated by the parameter  $R$ , and in the current method, it is the parameter  $\alpha$ .

As previously explained, the parameters used in the Olson et al. methodology were modified (in relation to the values recommended in the original article) in order to obtain consistent results. In the proposed method, on the other hand, the methodology provided satisfactory results except in set 6, where the filtering process has eliminated the

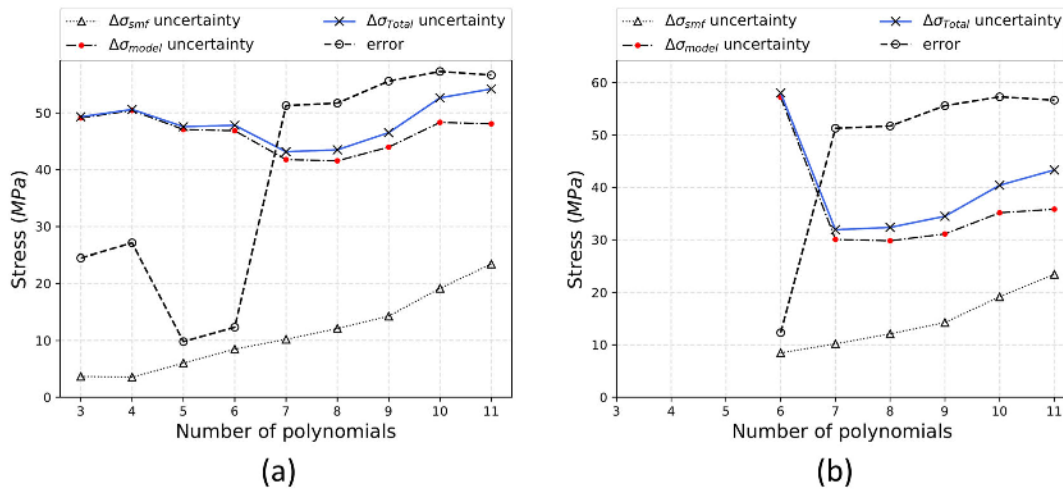


FIGURE 7 Solution for data set 6. (a) Before third sorting process. (b) After third sorting process.

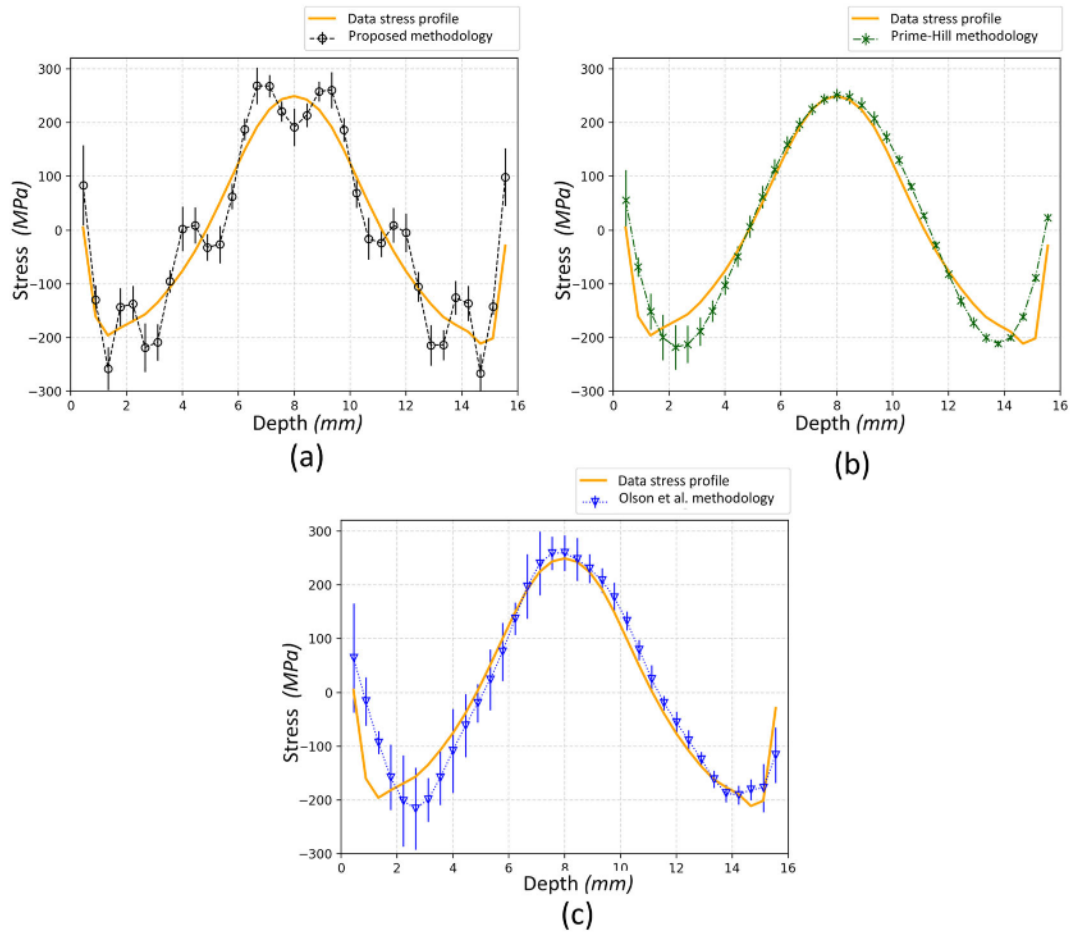


FIGURE 8 Set 6 residual stresses solutions. (a) Proposed methodology solution. (b) Prime-Hill methodology solution. (c) Olson et al. methodology solution.

options with the lowest error. Such difficulties are more important the higher the level of noise present. In this perspective, the results should always be compared as far as possible using different methodologies, in order to gain certainty of the answer. The new methodology, based on the results obtained, represents a valid methodology to be used (Figure 8).



In general, the methodology captures the evolution of the error when more polynomials are added into the solution, this is evidenced in the results of set 12 in Figure 4), where the data is free of noise. The uncertainty tends to increase when error increase and vice versa. The intensity of the rate of these changes is not always the same. This is why the minimum mean total uncertainty does not coincide with the minimum error. For the case of data sets number 2, 5, 7, 8 and 10, the minimum error is coincident with the minimum total uncertainty estimation, which shows the strong correlation between both of them.

Another advantage of the new methodology is that the solutions automatically satisfy equilibrium and are defined throughout the workpiece, which is especially useful for initialising residual stresses in a finite element model. However, its performance should be verified against the pulse regularisation method in fitting complicated stress distributions like in earlier studies.<sup>[16,21,22]</sup>

### 3.3.1 | Computational cost

Four parameters, maximum polynomial order, minimum polynomial order, minimum number of polynomials and maximum number of polynomials define the space of solutions that is going to be explored in the solution search. The computation cost and the quality of the answer depend on these variables.

The computation of the results presented in this section was obtained with a single Intel(R) Core(TM) i5-8350U processor. The biggest drawback of the presented methodology compared with the references is the computation cost, because it requires an intensive search in the space of solutions chosen by the user. The number of solutions to be evaluated may vary from a few hundred to millions.

Figure 9 presents the computational time consumption evolution for a different combinations of these two most relevant parameters.

Considering that the time axis is on a logarithmic scale, the computing time variates quickly from fraction of seconds to nearly an hour. By comparison, the other methods in the literature take only seconds.

It is not a simple task to predict the benefits obtained by exploring a wider space of solutions. Each problem is different, and the stress profile complexity determines the capacity of the basis be reproduced with a few or a large number of polynomials. Furthermore, a good fit will always be related to the following factors: the quality of the data and the capacity of the basis to reproduce the RSP. The wider the space explored, the better the likelihood of a better solution. For the particular case of this benchmark, exploring a wider space reduced the obtained error. Nevertheless, using a smaller space still gave good approximations with correct uncertainty estimation in fractions of seconds.

It is important to remark; this methodology may be applied to any other continuous expanded series. Legendre polynomials were used because they have the orthogonality property that increases data utilisation efficiency. This fact does not assure that solution lives in the space determined by the user. Furthermore, the use of higher-order polynomials may promote noise propagation.

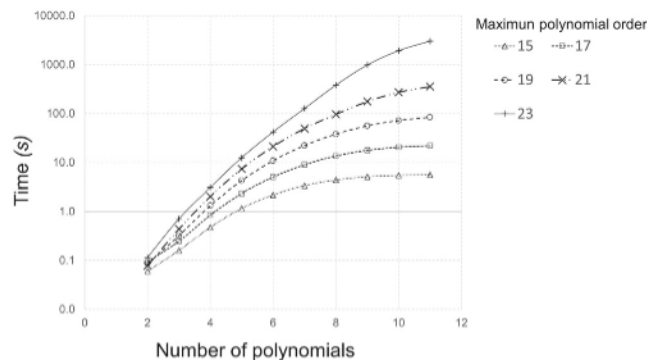


FIGURE 9 Computing time as function of parameters determining the space of solutions.

## 4 | CONCLUSION

A new iterative algorithm to calculate the residual stress field by inverse analysis on destructive tests using polynomials as the basis functions is proposed. Compared with previous work, this methodology explores a wider space of possible solutions. This is achieved by not requiring consecutive orders of polynomials in the basis functions. As a result, higher orders of polynomials are used without increasing the total number of polynomials in the solution. More complicated stress fields can be fit well than with previous methods based on series-expanded solutions.

Based on the statistical nature of the problem, a new methodology for estimating the model error component of total stress uncertainty is also proposed.

A benchmark test problem with a known solution was used to test the new methodology. The new method gave more accurate answers when tested on noisy data. An improvement in the accuracy of the uncertainty estimation was also achieved.

This new methodology is only limited by the computational cost. Compared with noncontinuous basis functions, it offers the advantage of obtaining an analytical and continuous solution that automatically satisfies equilibrium. It remains to study the effectiveness of the proposed new method under more complicated stress distribution conditions in order to verify whether the advantages obtained in this study are still valid.

## ACKNOWLEDGEMENTS

This work was supported in part by the I2M Laboratory of the University of Bordeaux and by the US Department of Energy through the Los Alamos National Laboratory. Los Alamos National Laboratory is operated by the Triad National Security, LLC, for the National Nuclear Security Administration of the US Department of Energy (contract no. 89233218CNA000001).

## DATA AVAILABILITY STATEMENT

The data that support the findings of this study are available from the corresponding author upon reasonable request.

## ORCID

Diego L. Brítez  <https://orcid.org/0000-0002-5424-4188>

## REFERENCES

- [1] G. S. Schajer, M. B. Prime, *J. Eng. Mater. Technol.* **2006**, 128(3), 375.
- [2] W. Cheng, I. Finnie, *Residual stress measurement and the slitting method*, Springer Science & Business Media **2007**.
- [3] M. B. Prime, M. R. Hill, *J. Eng. Mater. Technol.* **2006**, 128(2), 175.
- [4] M. B. Prime, V. C. Prantil, P. Rangaswamy, F. P. Garcia, *Mater. Sci. Forum*, **2000**, 347-349, 223.
- [5] S. D. Salehi, M. M. Shokrieh, *Int. J. Mech. Sci.* **2019**, 152, 558.
- [6] T. C. Smit, R. G. Reid, *Exper. Mech.* **2018**, 58(8), 1221.
- [7] R. G. Treuting, W. T. Read Jr, *J. Appl. Phys.* **1951**, 22, 130.
- [8] G. S. Schajer, *J. Eng. Mater. Technol.* **1988**, 110(4), 338.
- [9] G. S. Schajer, E. Altus, *J. Eng. Mater. Technol.* **1996**, 118(1), 120.
- [10] G. S. Schajer, *Exper. Mech.* **2010**, 50(2), 159.
- [11] W. Cheng, I. Finnie, O. Vadar, *J. Eng. Mater. Technol.* **1991**, 113(2), 199.
- [12] W. Cheng, M. B. Prime, I. Finnie, *Residual Stress.: Sci. Technol.* **1991**, 2, 1127.
- [13] M. R. Hill, *Practical residual stress measurement methods: The slitting method*, Wiley Online Library **2013**.
- [14] M. B. Prime, *Appl. Mech. Rev.* **1999**, 52(2), 75.
- [15] F. Hosseinzadeh, M. Burak Toparli, P. Bouchard, *J. Press. Vessel Technol.* **2012**, 134(1), 011402.
- [16] M. Strantza, B. Vrancken, M. B. Prime, C. E. Truman, M. Rombouts, D. W. Brown, P. Guillaume, D. Van Hemelrijck, *Acta Materialia* **2019**, 168, 299.
- [17] M. Weiss, B. Rolfe, P. D. Hodgson, C. Yang, *J. Mater. Process. Technol.* **2012**, 212(4), 877.
- [18] M. De Giorgi, *Int. J. Fatigue* **2011**, 33(3), 507.
- [19] R. A. Mayville, I. Finnie, *Exper. Mech.* **1982**, 22, 197.
- [20] M. D. Olson, A. T. DeWald, M. R. Hill, *Exper. Mech.* **2020**, 60(1), 65.
- [21] W. Wong, M. R. Hill, *Exper. Mech.* **2013**, 53(3), 339.
- [22] J. A. Ronevich, C. R. D'Elia, M. R. Hill, *Eng. Fracture Mech.* **2018**, 194, 42.

**How to cite this article:** D. L. Brítez, M. B. Prime, S. Werda, R. Laheurte, P. Darnis, O. Cahuc, *Strain* 2023, 59(1), e12430. <https://doi.org/10.1111/str.12430>

## APPENDIX A: UNCERTAINTIES AND ERROR COMPARISON OF DIFFERENT DATA SETS

The following figures represent the mean error through the thickness and the total uncertainty as well as its components (stress uncertainty due to model error and to strain misfit) before (left figures) and after (right figures) for each set of data sets not presented in the main text.

Observation: In this particular case of set 1, the third sorting procedure did not eliminate any possible solution of the set; this is why both solutions (before and after this step) are identical.

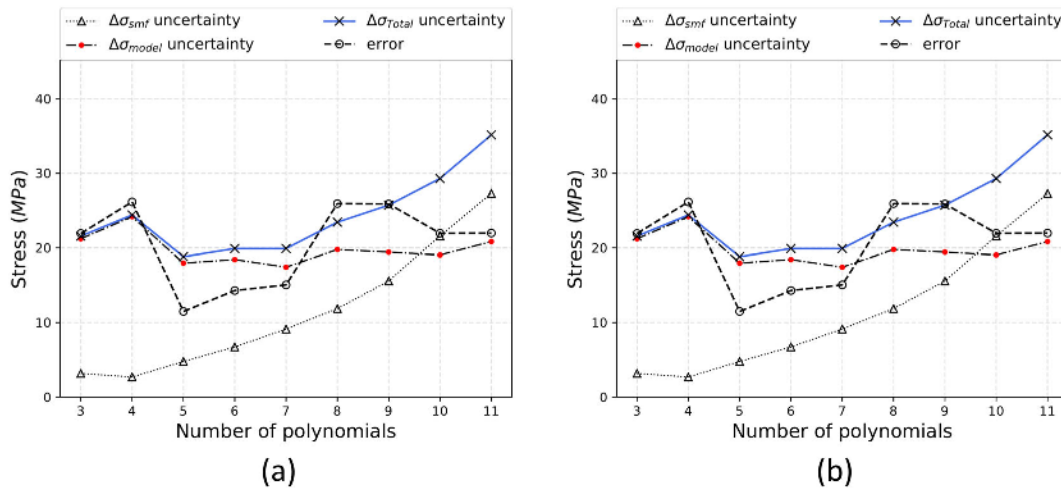


**FIGURE A1** Solution for data set 1. (a) Before third sorting process. (b) After third sorting process

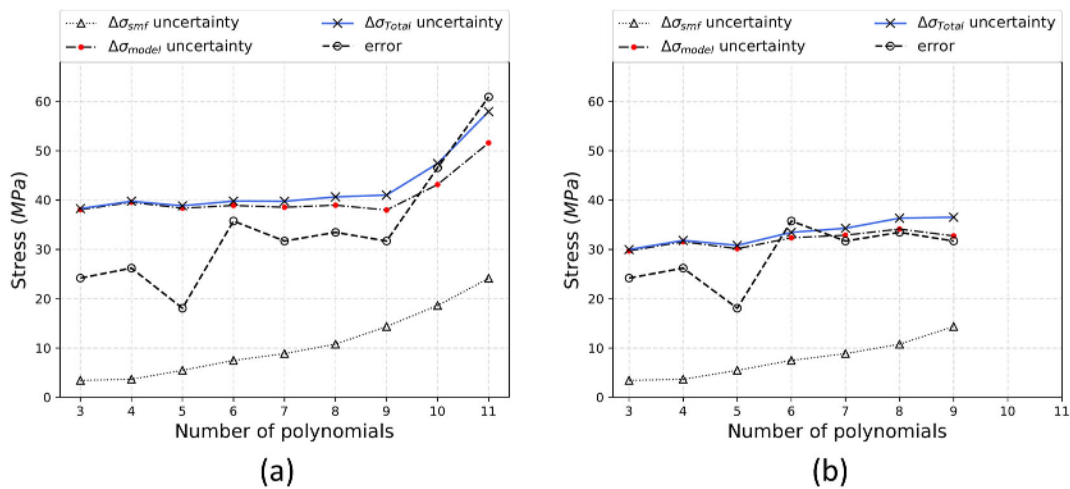


**FIGURE A2** Solution for data set 2. (a) Before third sorting process. (b) After third sorting process



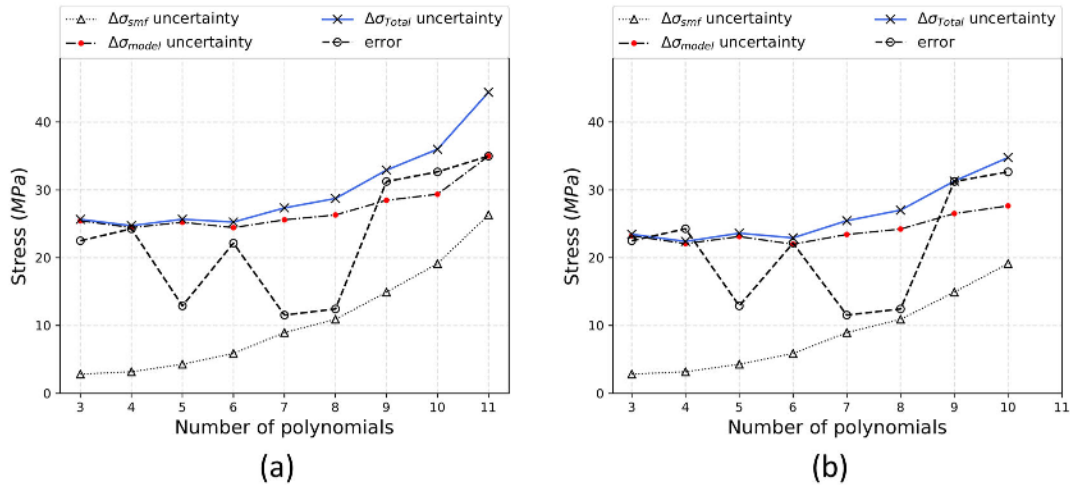


FIGURE A3 Solution for data set 4. (a) Before third sorting process. (b) After third sorting process

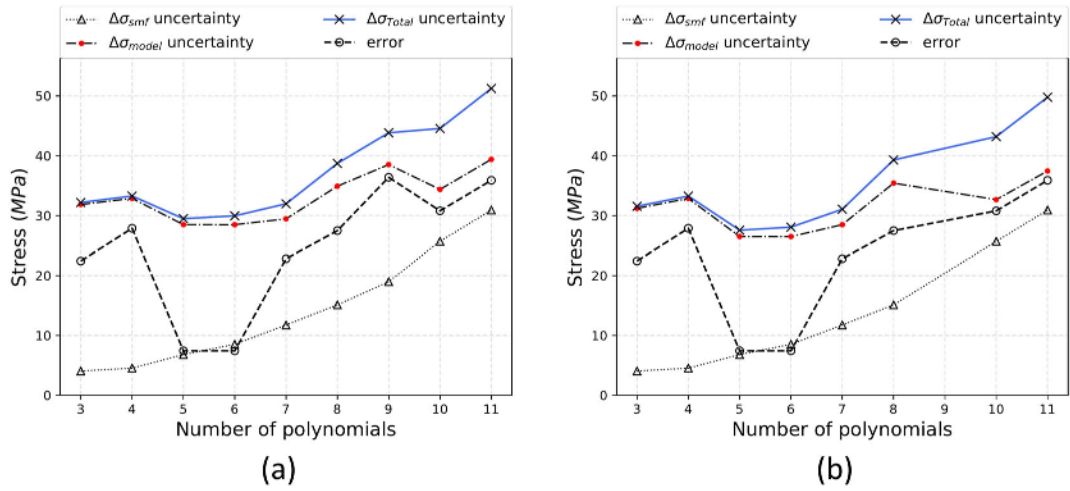


FIGURE A4 Solution for data set 5. (a) Before third sorting process. (b) After third sorting process

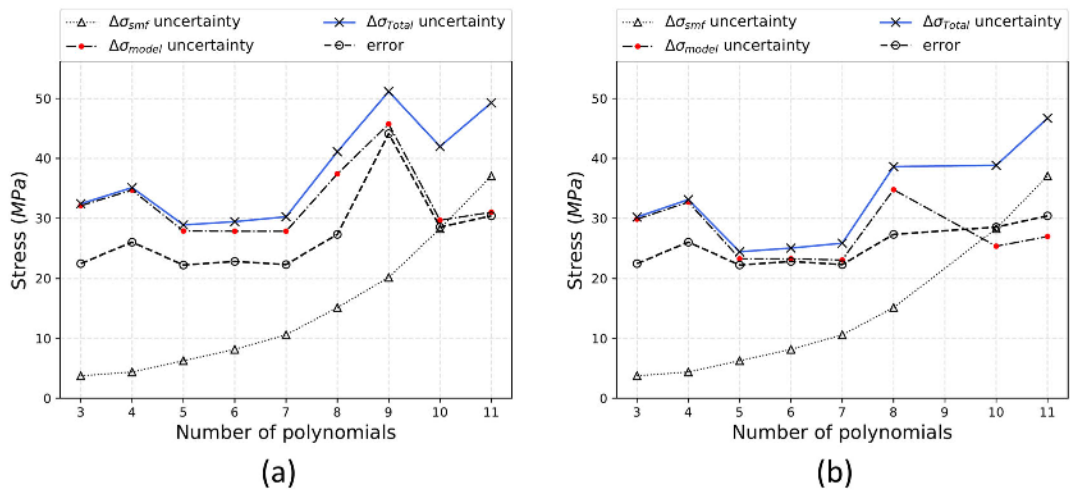


FIGURE A5 Solution for data set 7. (a) Before third sorting process. (b) After third sorting process

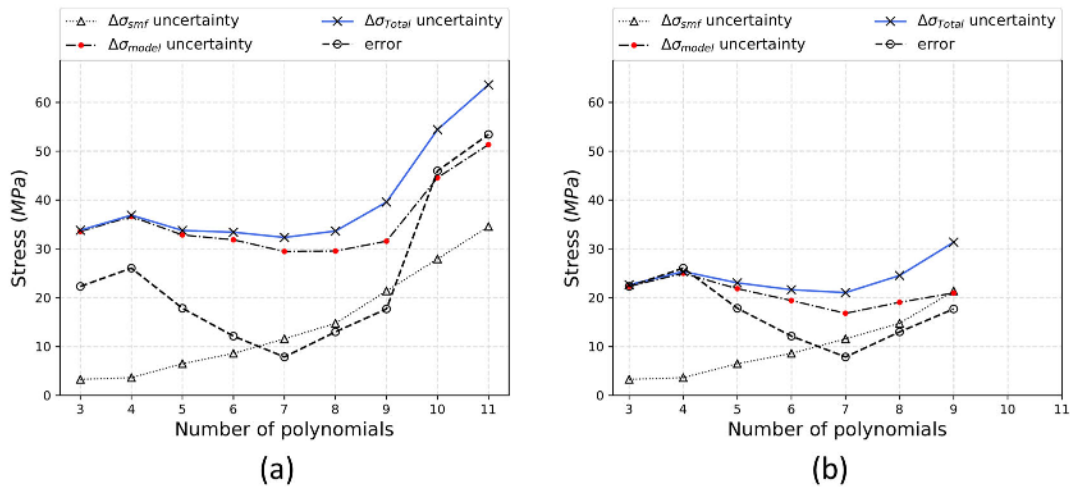


FIGURE A6 Solution for data set 8. (a) Before third sorting process. (b) After third sorting process

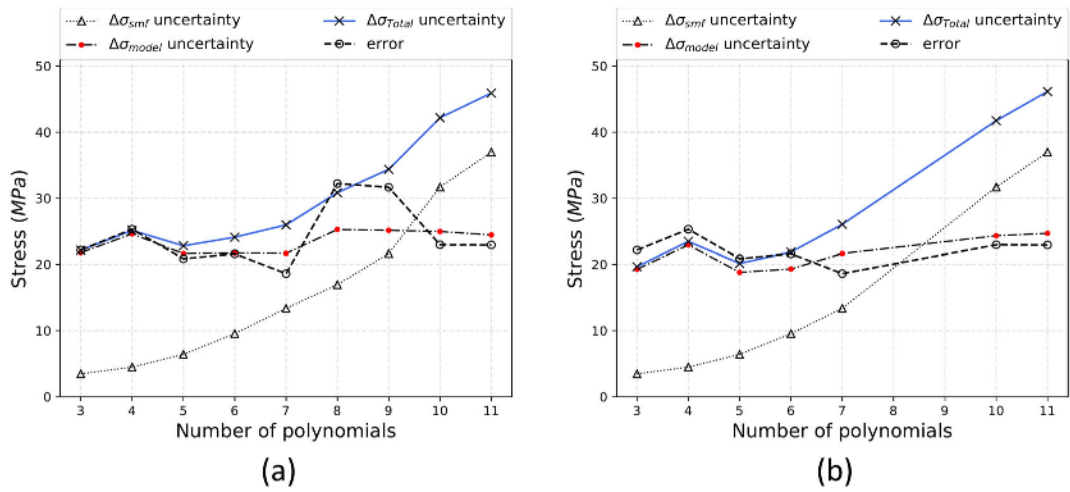


FIGURE A7 Solution for data set 9. (a) Before third sorting process. (b) After third sorting process

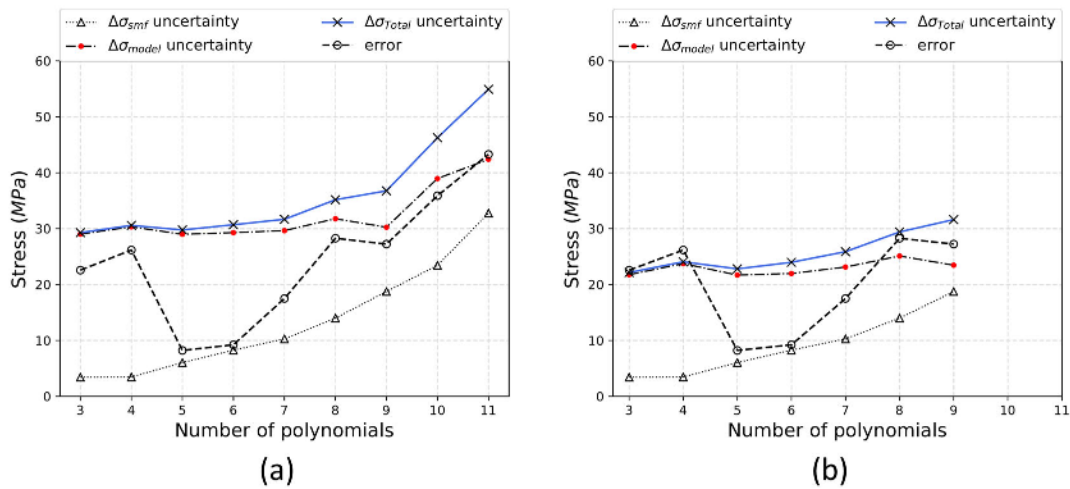
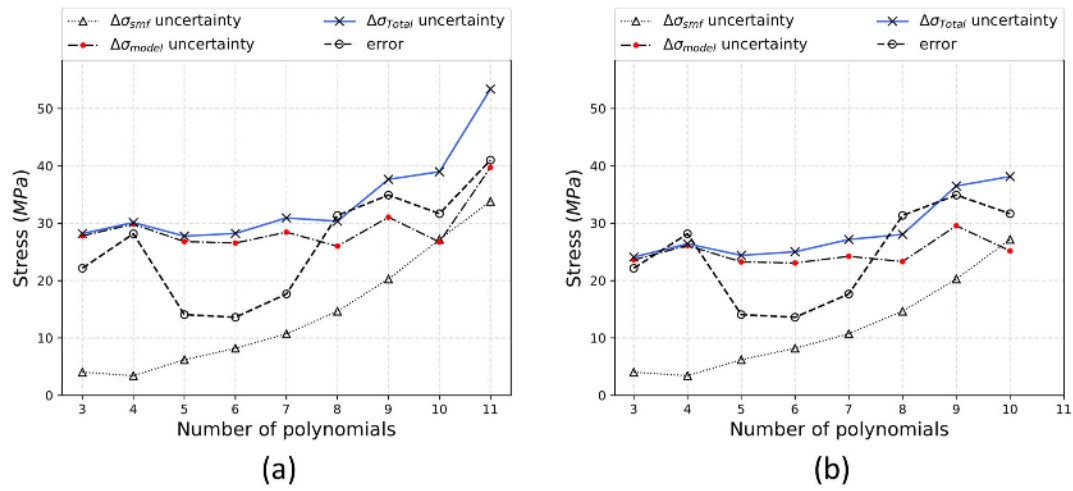


FIGURE A8 Solution for data set 10. (a) Before third sorting process. (b) After third sorting process



**FIGURE A9** Solution for data set 11. (a) Before third sorting process. (b) After third sorting process



## APPENDIX B: ALGORITHM CHART

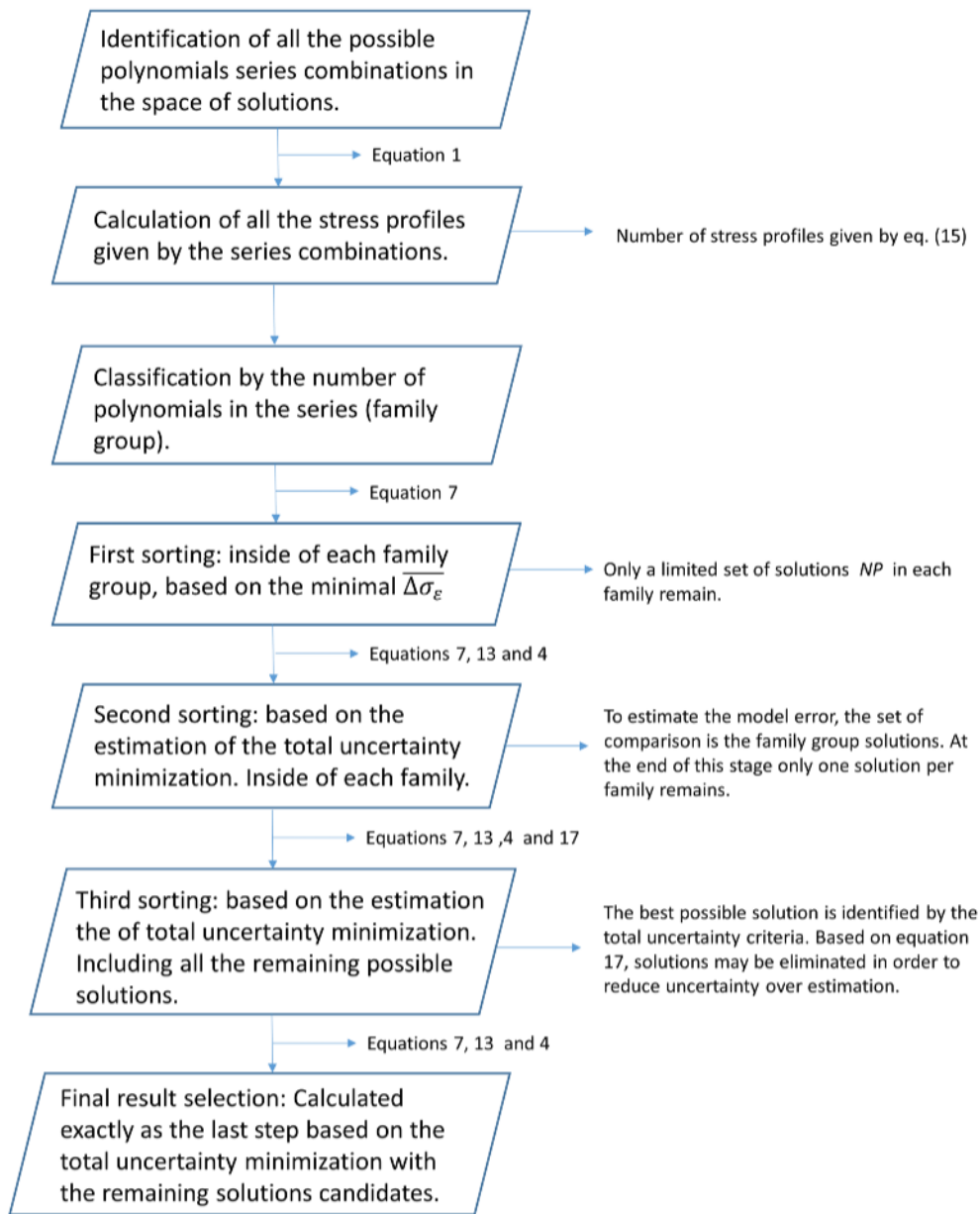


FIGURE B1 Algorithm chart